Inorganic Chemistry

Article

pubs.acs.org/IC

Aryl-Linked Salicylaldoxime-Based Copper(II) Helicates and "Boxes": Synthesis, X-ray Analysis, and Anion Influence on Complex Structure

Ajay Pal Singh Pannu, James R. Stevens, and Paul G. Plieger*

Institute of Fundamental Sciences, Massey University, Private Bag 11 222, Palmerston North, New Zealand

Supporting Information

ABSTRACT: The synthesis and spectroscopic analysis of both "metal-only" and anion encapsulated salicylaldoxime-based complexes utilizing a new 1,3-xylyl strap are described. X-ray crystallographic analysis reveals that the aromatic spacer restricts the confirmation flexibility of the resulting complexes leading to dicopper(II) double helicate and dicopper(II) 2 + 2 "box" structural forms. The choice of the structural motif is influenced by the anion present, with the copper(II) nitrate-containing complex $[NO_3{\subset}(Cu_2\mathbf{L}^3_2)](NO_3)_3$, **4**, adopting a double helicate form, whereas the analogous copper(II) bromide complexes $[2Br{\subset}(Cu_2\mathbf{L}^3_2)](Br)_2$, **5**, and $[2Br{\subset}(Cu_2\mathbf{L}^3_2)](BF_4)_2$, **6**, both adopt 2 + 2 "box" structural configurations. Spectroscopic analysis has shown an enhancement in the binding strength of ClO_4^- over the anions SO_4^{2-} and NO_3^-. The enhanced rigidity caused by the use of the 1,3-xylyl spacer in this series of complexes has favored the formation of the "double loaded" dibromide complex.

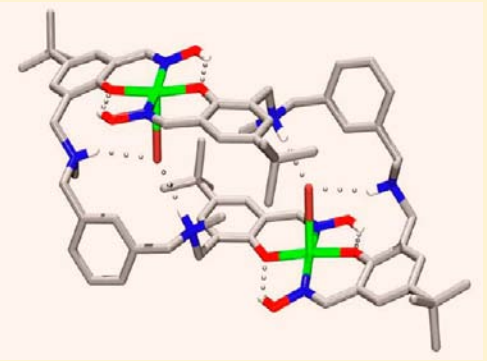

INTRODUCTION

Over the last few decades, the field of selective anion recognition has attracted much attention and has developed rapidly as a subdiscipline of supramolecular chemistry. The initiative taken by Park and Simmons to describe how simple bicyclic diaza katapinanda could encapsulate halide ions[1] marked the birth of "anion coordination chemistry". This work inspired many efforts into the research of ammonium and polyammonium-based anion receptors around that time.[2] Hydrogen bonding and/or electrostatic interactions coupled with topological complementarity between protonated amines and the anion guests govern the binding in these systems. A number of researchers are now involved in this fast evolving field, which includes a wide variety of different types of amine- or ammonium-based receptors.[3] Among such systems, the synthesis of ditopic receptors designed for simultaneous binding of both cations and their attendant anions is a further challenging task due to the specific requirements needed to be met by both the metal coordinating site and the anion binding site/pocket.[4] Nevertheless, such innovative and well-designed receptors have been reported on a regular basis.[5]

In the past few years, we have been actively designing new polyammonium-based ditopic receptors and exploring the use of dicopper(II) helical complexes of these new ligands as anion binding receptors.[6,7] Our design consists of utilizing salicylaldimine[6] or salicylaldoxime[7] functionality for metal coordination; these groups are then in turn linked together via straps of alkyl ($\mathbf{L}^1$ in Scheme 1) or aromatic ($\mathbf{L}^2$ in Scheme 1) tertiary amines. Coordination of these ligands to metal salts results in the formation of neutral dimetallic helicates with metal(II) centers coordinated to phenoxide oxygen and oxime nitrogen atoms. In the absence of a suitably alkaline metal salt, this process results in the protonation of the tertiary amine sites within the newly formed cage complex, thus enabling the receptor to form both hydrogen bonds, electrostatic interactions, and (in some cases) metal covalent bonds with encapsulated anions.[6,7] In the course of this work, we have observed that the uptake of an anion within the helical cage leads to a major contraction of the complex bringing the two metal centers closer to one another.[7a] Further studies among these complexes have shown selective uptake of sulfate over dihydrogen phosphate in aqueous media,

Scheme 1. General Form of the Ligands Used To Make the Dicopper Helicates

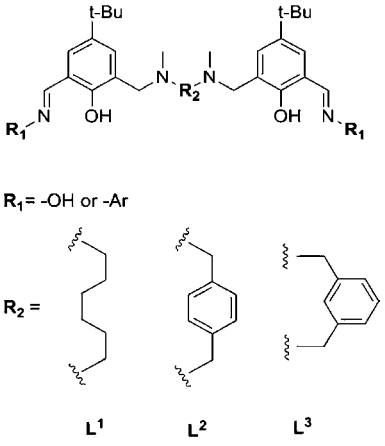

Received: April 9, 2013
Published: August 8, 2013

   dx.doi.org/10.1021/ic400829d | Inorg. Chem. 2013, 52, 9327−9337

Scheme 2

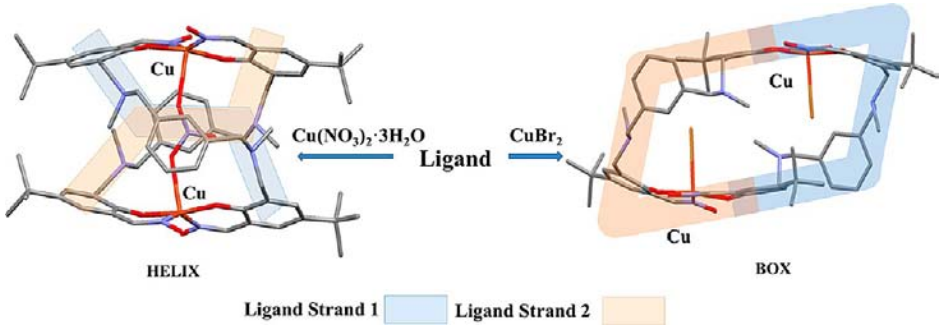

whereas no major changes were observed in nonaqueous media.[7b] It has also been shown that deprotonation of the oxime functionality within ligands of this type during complexation leads to the formation of triple helicate complexes with expanded trimetallic cores.[8]

We have shown that a decrease in ligand conformational flexibility can lead to an enhancement in anion binding strength, for example, substitution of the flexible six-carbon alkyl strap ($\mathbf{L}^1$, Scheme 1) with that of a six carbon aromatic *p*-xylylic spacer ($\mathbf{L}^2$, Scheme 1).[7c] This minor change has led to a clear enhancement in the binding strength of sulfate over other noncoordinating anions. In the present work, we go a step further to analyze similar results by replacing the *p*-xylylic spacer with a *m*-xylylic one ($\mathbf{L}^3$, Scheme 1). This change in structural rigidity has resulted in dramatic effects on the geometry adopted by the complexes as well as their anion binding preferences when compared to the analogous *p*-xylylic linker-based ones.

Two of the main factors that affect the geometry and arrangement of supramolecular inorganic complexes are the metal coordination preferences and the ligand structure. A third and sometimes overlooked additional factor is the role that the counterion (anion) plays in the construction and form of the resulting complexes.[9] This templating effect of anions on the resulting structure is far less documented as compared to the other two factors due to the intrinsic properties of anions such as their diffuse nature, pH sensitivity, and high solvation free energies. Dunbar and co-workers highlighted this "anion template effect" in depicting the resulting structural motifs among M(II)−bptz complexes, where judicious choice of anion resulted in the formation of either a molecular square or a pentagon (where M = Ni, Zn and bptz = 3,6-bis(2pyridyl)-1,2,4,5-tetrazine).[9b] Lee et al. reported that anion size can regulate the secondary structure of a coordination chain, from folded helical, cyclic, to unfolded linear chain conformations in the solid state.[9c] More recently, in 2013, Beer et al. have summarized their efforts in the area of anion influenced syntheses of interlocked structures, demonstrating the versatility and scope of this approach.[9d] In the present work, the use of $Cu(NO_3)_2{\cdot}3H_2O$ metal salt leads to the formation of a dicopper(II) double helicate structure $[NO_3{\subset}(Cu_2\mathbf{L}^3_2)](NO_3)_3$, **4**, whereas the use of bromide and bromide/tetrafluoroborate Cu(II) salts resulted in $[2Br{\subset}(Cu_2\mathbf{L}^3_2)](Br)_2$, **5**, and $[2Br{\subset}(Cu_2\mathbf{L}^3_2)](BF_4)_2$, **6**, dicopper(II) 2 + 2 "boxes", respectively showing the strong influence of anion on the structural forms adopted by the resulting complex (Scheme 2).

EXPERIMENTAL SECTION

Unless specified, commercial reagents and solvents were used without purification. ^{1}H and ^{13}C NMR spectra were recorded on Bruker Avance 400 and 500 MHz spectrometers; δ values are relative to TMS or the corresponding solvent. Mass spectra were obtained using a Micromass ZMD 400 electrospray spectrometer. IR spectra were recorded on a Nicolet 5700 FT-IR spectrometer from Thermo Electron Corp. using an ATR sampling accessory. UV−vis spectra were recorded in THF using a CARY 100Bio UV−vis spectrometer. Elemental analyses were determined by the Campbell Microanalytical Laboratory at the University of Otago.

Synthesis of the Ligands. Ligand $\mathbf{L}^3$ was prepared from the corresponding aromatic dialdehyde in a manner analogous to that described for $\mathbf{L}^2$.[7c]

*N,N′-Dimethyl-m-xylylenediamine (**1a**).* A solution of methylamine hydrochloride (0.877 g, 13.0 mmol) in methanol (40 mL) was allowed to react with a solution of potassium hydroxide (0.808 g, 14.4 mmol) in methanol (40 mL). The filtered solution was added dropwise into a second solution of isophthalaldehyde (0.522 g, 3.89 mmol) in methanol (40 mL) over 1 h. The pale yellow solution was then stirred at room temperature for 2 h. Sodium borohydride (0.314 g, 8.30 mmol) was added portionwise to the stirred solution over 10 min and left to stir for 2 h. The solvent was removed under reduced pressure, and the resulting white solid was dissolved in chloroform (40 mL) and washed with water (40 mL). The organic layer was separated, dried over anhydrous $MgSO_4$, and the solvent was removed in vacuo, leaving a pale yellow oil, **1a** (0.608 g, 95%). δ_H (500 MHz; $CDCl_3$; Me_4Si): 7.28 (2H, m, Ar*H*), 7.20 (2H, dd, J = 1.7, 6.9 Hz, Ar*H*), 3.74 (4H, s, CH_2), 2.45 (6H, s, CH_3). δ_C (125 MHz; $CDCl_3$; Me_4Si): 140.4 (Ar*C*), 128.6 (Ar*C*H), 128.2 (Ar*C*H), 127.0 (Ar*C*H) 56.2 (*C*H$_2$), 36.2 (*C*H$_3$). Anal Calcd for $C_{10}H_{16}N_2{\cdot}0.6H_2O$: C, 68.61; H, 9.90; N, 16.00. Found (%): C, 68.57; H, 9.58; N, 15.82. m/z (ESI) 165.45 (**1a**)$^+$. IR υ_{max} (KBr)/cm^{-1}: 3293 (N−H), 2787m (C−H), 783s, 701s (Ar−H).

*3,3′-(1,3-Phenylenebis(methylene))bis(methylazanediyl)bis-(methylene)bis(5-tert-butyl-2-hydroxybenzaldehyde) (**1b**).* To a stirred solution of triethylamine (0.900 g, 8.89 mmol) in dichloromethane (60 mL) were added simultaneously and slowly solutions of 3-(bromomethyl)-5-*tert*-butyl-2-hydroxybenzaldehyde (2.007 g, 7.42 mmol) in dichloromethane (80 mL) and *N,N′*-dimethyl-*m*-xylylenediamine **1a** (0.608 g, 3.75 mmol) in dichloromethane (80 mL) over 1 h. The reaction was monitored for completion via ^{1}H NMR and was completed in 3 h. The solvent was reduced in volume (50 mL) and the organic layer washed with water (2 × 20 mL), separated, and dried over anhydrous $MgSO_4$. The solvent was removed under reduced pressure, and the product was dissolved in ethyl acetate and isolated by diethyl ether diffusion. The product was collected and washed with diethyl ether and dried in vacuo to give a yellow solid (0.807 g, 41%). δ_H (500 MHz; $CDCl_3$; Me_4Si): 10.30 (2H, s, C*H*O), 7.61 (2H, d, J = 2.2 Hz, Ar*H*), 7.38 (2H, d, J = 1.7 Hz, Ar*H*), 7.35 (1H, t, J = 7.4 Hz, Ar*H*), 7.28 (1H, s, Ar*H*), 7.26 (2H, d, J = 7.1 Hz, Ar*H*), 3.76 (4H, s, CH_2), 3.64 (4H, s, CH_2), 2.29 (6H, s, NCH_3), 1.30 (18H, s, C(CH_3)$_3$). δ_C (100 MHz; $CDCl_3$; Me_4Si): 192.5 (*C*HO), 159.3 (*C*OH), 142.1 (Ar*C*), 137.6 (Ar*C*), 133.3 (Ar*C*H), 130.4 (Ar*C*H), 129.1 (Ar*C*H), 128.8 (Ar*C*H), 125.2 (Ar*C*H), 123.9 (Ar*C*), 122.0

dx.doi.org/10.1021/ic400829d | Inorg. Chem. 2013, 52, 9327−9337

Table 1. Crystal Data and Structure Refinement for L^3, 1, 4, 5, and 6

	L^3	1	4	5	6
empirical formula	$C_{34}H_{46}N_4O_4$	$C_{40}H_{58}CuN_4O_5$	$C_{68}H_{92}Cu_2N_{12}O_{20}$	$C_{70}H_{98}Br_4Cu_2N_8O_{10}$	$C_{210}H_{288}B_6Br_6Cu_6F_{24}N_{24}O_{26}$
formula weight	574.75	738.44	1524.62	1658.28	4946.20
crystal system, space group	monoclinic, *C*2/*c*	triclinic, $P\bar{1}$	monoclinic, P21	monoclinic, *P*21/*c*	triclinic, $P\bar{1}$
a (Å)	25.7501(9)	11.5153(14)	11.4408(19)	22.7715(16)	14.5994(12)
b (Å)	8.7686(3)	13.7564(17)	20.2715(4)	19.5276(4)	19.6925(17)
c (Å)	14.9082(12)	14.434(2)	19.0446(13)	19.8252(4)	27.748(2)
α (deg)	90	78.740(6)	90	90	99.607(7)
β (deg)	113.157(17)	69.547(5)	106.297(10)	93.245(7)	96.215(7)
γ (deg)	90	68.645(5)	90	90	106.635(7)
volume (Å^3)	3094.9(3)	1989.2(4)	4239.4(8)	8801.6(7)	7433.0(11)
Z	4	2	2	4	1
reflns collected/ unique	16 396/2992 [*R*(int) = 0.0869]	24 934/6519 [*R*(int) = 0.0675]	49 913/14 261 [*R*(int) = 0.0559]	90 481/16 757 [*R*(int) = 0.0691]	73 025/20 103 [*R*(int) = 0.1243]
data/restraints/ parameters	2992/42/232	519/0/452	14 261/721/940	16 757/12/860	20 103/1070/1408
GOF on F^2	1.030	1.142	1.097	1.114	0.874
final *R* indices [$I > 2\sigma(I)$]	R_1 = 0.0799, wR_2 = 0.2075	R_1 = 0.0530, wR_2 = 0.1358	R_1 = 0.0724, wR_2 = 0.1867	R_1 = 0.0563, wR_2 = 0.1581	R_1 = 0.1108, wR_2 = 0.2732
R indices (all data)	R_1 = 0.1367, wR_2 = 0.2603	R_1 = 0.0891, wR_2 = 0.1585	R_1 = 0.0971, wR_2 = 0.2287	R_1 = 0.0760, wR_2 = 0.1789	R_1 = 0.2414, wR_2 = 0.3336
CCDC no.	926413	926414	926417	926415	926416

(Ar*C*), 61.6 (*C*H$_2$), 58.8 (*C*H$_2$), 41.8 (*C*H$_3$), 34.3 (*C*(CH$_3$)$_3$), 31.5 (C(*C*H$_3$)$_3$). Anal. Calcd for $C_{34}H_{44}N_2O_4\cdot0.5H_2O$: C, 73.75; H, 8.19; N, 5.06. Found: C, 74.03; H, 8.02; N, 4.83. *m*/*z* (ESI) 545.93 (**1b**)$^+$. IR υ_{max} (KBr)/cm^{-1}: 2958br (C−H), 1678s (C═O), 1217s (C−O), 746m, 731m (Ar−H).

*(1E,1′E)-5-tert-Butyl-3-((((3-(((5-tert-butyl-2-hydroxy-3-((E)-(hydroxyimino)methyl)benzyl)(methyl)amino)methyl)benzyl)-(methyl)amino)methyl)-2-hydroxybenzaldehyde Oxime (**L**^{3}).* A solution of hydroxylamine hydrochloride (0.714 g, 10.28 mmol) in ethanol (50 mL) was allowed to mix with a solution of potassium hydroxide (0.610 g, 10.87 mmol) in ethanol (50 mL). The resulting white precipitate was removed by filtration. The filtered solution was slowly dripped into a solution of **1b** (1.851 g, 3.40 mmol) in ethanol (100 mL) over 2 h. The pale yellow solution was then allowed to stir at room temperature overnight. The solution was removed under reduced pressure, dissolved in chloroform (50 mL), and washed with water (2 × 20 mL). The organic layer was separated and dried over anhydrous MgSO$_4$. The solvent was removed under reduced pressure, and the product was dissolved in ethyl acetate and precipitated using hexane diffusion. The product was collected and washed with diethyl ether and dried in vacuo to give a white solid (0.980 g, 50%). δ_H (400 MHz; CDCl$_3$; Me$_4$Si): 10.16 (2H, br s, NO*H*), 8.44 (2H, s, C*H*NOH), 7.41 (2H, d, *J* = 2.2 Hz, Ar*H*), 7.33−7.27 (4H, m, Ar*H*), 7.13 (2H, d, *J* = 2.0 Hz, Ar*H*), 3.74 (4H, s, C*H*$_2$), 3.66 (4H, s, C*H*$_2$), 2.27 (6H, s, NC*H*$_3$), 1.29 (18H, s, C(C*H*$_3$)$_3$). δ_C (100 MHz; CDCl$_3$; Me$_4$Si): 154.3 (*C*OH), 148.7 (*C*HNOH), 141.7 (Ar*C*), 137.2 (Ar*C*), 130.7 (Ar*C*H), 128.9 (Ar*C*H), 128.3 (Ar*C*H), 124.0 (Ar*C*H), 122.5 (Ar*C*), 117.7 (Ar*C*), 61.5 (*C*H$_2$), 59.3 (*C*H$_2$), 41.6 (*C*H$_3$), 34.1 (*C*(CH$_3$)$_3$), 31.6 (C(*C*H$_3$)$_3$). Anal. Calcd for $C_{34}H_{46}N_4O_4\cdot0.5H_2O\cdot0.5C_6H_{14}$: C, 70.89; H, 8.68; N, 8.94. Found: C, 71.01; H, 8.36; N, 8.86. *m*/*z* (ESI) 575.47 [**L**^{3} + H]$^+$. IR υ_{max} (KBr)/cm^{-1}: 2960br (C−H), 1613brw (C═N), 1266s (C−O), 750s, 712s (Ar−H); mp 168.5−171.0°.

*General Cu(II) Complex Synthesis with **L**^{3}.* To a stirred pale yellow solution of **L**^{3} (9.0 mmol L^{-1}) in methanol (40 mL) was slowly added dropwise 1 mole equivalent of the copper(II) salt (9.0 mmol L^{-1}) in methanol in (40 mL) over 30 min. The resulting colored solution was stirred for 20 h. The solvent was evaporated to dryness. The crude product was then purified by recrystallization.

*"Copper-Only" Complex, [Cu$_2$(**L**^{3}-2H)$_2$], **1**.* The general method outlined above was followed using copper(II) acetate monohydrate. The crude brown product was purified by recrystallization with diisopropyl ether diffusion from a tetrahydrofuran/chloroform (1:1) mix to afford brown platelet crystals. The crystals were collected and washed with diethyl ether (0.655 g, 29%). Anal. Calcd for $C_{68}H_{88}N_8O_8Cu_2$: C, 64.18; H, 6.97; N, 8.81. Found: C, 63.92; H, 7.06; N, 8.67. *m*/*z* (ESI) 636.79 [(**L**^{3}-H)Cu]$^+$. UV−vis (THF, 1.5 × 10^{-5} mol L^{-1}) λ_{max}/nm (ε/L mol^{-1} cm^{-1}): 355 (19 800), 272 (57 300), 255 (74 900). IR υ_{max} (KBr)/cm^{-1}: 3140brw (O−H), 1630m (C═N), 766w, 714s (Ar−H).

*[SO$_4$⊂(Cu$_2$**L**^{3}$_2$)]SO$_4$, **2**.* The general method outlined above was followed using copper(II) sulfate pentahydrate. The green product was purified by recrystallization with diethyl ether diffusion from DMF. The product was collected and washed with diethyl ether (0.078 g, 21%). Anal. Calcd for $C_{68}H_{92}N_8O_{24}S_4Cu_2\cdot7H_2O\cdot$DMF: C, 51.13; H, 6.83; N, 7.56. Found: C, 51.22; H, 6.42; N, 7.54. *m*/*z* (ESI-HR) 636.2697 [**L**^{3}CuH]$^+$, 1273.5306 [(**L**^{3})$_2$Cu$_2$H]$^+$. UV−vis (THF/0.5% MeOH, 2.0 × 10^{-5} mol L^{-1}) λ_{max}/nm (ε/L mol^{-1} cm^{-1}): 359 (17 000). IR υ_{max} (KBr)/cm^{-1}: 1629brm (C═N), 1106brs, 1035brs (SO$_4$), 712m (Ar−H).

*[ClO$_4$⊂(Cu$_2$**L**^{3}$_2$)](ClO$_4$)$_3$, **3**.* The general method outlined above was followed using copper(II) perchlorate hexahydrate. The product was purified by recrystallization with diethyl ether diffusion from methanol. The brown product was collected and washed with diethyl ether (0.033 g, 25%). Anal. Calcd for $C_{68}H_{92}N_8O_{24}Cl_4Cu_2\cdot4H_2O$: C, 46.77; H, 5.77; N, 6.42. Found: C, 46.59; H, 5.61; N, 6.31. *m*/*z* (ESI) 736.67 ([ClO$_4$**L**^{3}Cu])$^+$. UV−vis (THF/0.1% MeCN, 2.0 × 10^{-5} mol L^{-1}) λ_{max}/nm (ε/L mol^{-1} cm^{-1}): 353 (16 700), 271 (43 200). IR υ_{max} (KBr)/cm^{-1}: 1620m (C═N), 1097brs (ClO$_4$), 710s (Ar−H).

*[NO$_3$⊂(Cu$_2$**L**^{3}$_2$)](NO$_3$)$_3$, **4**.* The general method outlined above was followed using copper(II) nitrate trihydrate. The dark green product was purified by recrystallization with diisopropyl ether diffusion from methanol to afford both green block and rod crystals that had identical composition. The crystals were collected and washed with diisopropyl ether (0.065 g, 20%). Anal. Calcd for $C_{68}H_{92}N_{12}O_{20}Cu_2\cdot3H_2O$: C, 51.74; H, 6.26; N, 10.65. Found: C, 51.91; H, 6.18; N, 10.61. *m*/*z* (ESI) 699.40 ([NO$_3$**L**^{3}Cu])$^+$. UV−vis (THF/0.3% MeCN, 2.0 × 10^{-5} mol L^{-1}) λ_{max}/nm (ε/L mol^{-1} cm^{-1}): 362 (12 400), 273 (36 500). IR υ_{max} (KBr)/cm^{-1}: 1627s (C═N), 1304brs (NO$_3$), 837m, 712s (Ar−H).

*[2Br⊂(Cu$_2$**L**^{3}$_2$)](Br)$_2$, **5**.* The general method outlined above was followed using copper(II) bromide. The dark brown product was purified by recrystallization with chloroform diffusion from a methanol/acetone (1:1) mix to afford green block crystals. The dark green crystals were collected and washed with diethyl ether (0.102 g, 22%). Anal. Calcd for $C_{68}H_{92}N_8O_8Br_4Cu_2\cdot4H_2O$: C, 48.96; H, 6.04; N,

dx.doi.org/10.1021/ic400829d | Inorg. Chem. 2013, 52, 9327−9337

6.72. Found: C, 48.68; H, 5.75; N, 6.82. *m/z* (ESI) 718.73 ($[BrL^3Cu]^+$). UV−vis (THF/0.4% MeCN, 2.0×10^{-5} mol L^{-1}) λ_{max}/nm (ε/L mol^{-1} cm^{-1}): 366 (10 200), 285 (24 900). IR υ_{max} (KBr)/cm^{-1}: 1611w (C═N), 710s (Ar−H).

[2Br⊂(Cu$_2$L$^3_2$)](BF$_4$)$_2$, **6**. The general method outlined above was followed using copper(II) tetrafluoroborate monohydrate and stirring for 1 h. This was then followed by the slow addition of 0.5 mole equivalents of *t*-butyl ammonium bromide (TBABr) in methanol (20 mL) and left to stir for 20 h. The product was purified by recrystallization with diethyl ether diffusion from a methanol/acetone (1:1) mix to afford green platelets and block crystals. The green crystals were collected and washed with diethyl ether (0.050 g, 35%). Anal. Calcd for $C_{68}H_{92}N_8O_8Br_2B_2F_8Cu_2$: C, 50.73; H, 5.76; N, 6.96. Found: C, 50.68; H, 6.07; N, 6.75. *m/z* (ESI) 718.73 ($[BrL^3Cu]^+$). UV−vis (THF/0.2% MeCN, 2.0×10^{-5} mol L^{-1}) λ_{max}/nm (ε/L mol^{-1} cm^{-1}): 367 (14 300), 285 (29 200). IR υ_{max} (KBr)/cm^{-1}: 1611w (C═N), 1058brs (BF_4), 710s (Ar−H).

X-ray Structure Determination. X-ray data of ligand L^3 and complexes **1**, **4**, **5**, and **6** were recorded at low temperature with a Rigaku-Spider X-ray diffractometer, comprising a Rigaku MM007 microfocus copper rotating-anode generator, high-flux Osmic monochromating and focusing multilayer mirror optics (Cu K radiation, λ = 1.5418 Å), and a curved image-plate detector. CrystalClear[10a] was utilized for data collection and FSProcess in PROCESS-AUTO[10b] for cell refinement and data reduction. All structures were solved employing direct methods and expanded by Fourier techniques.[10c] Non-hydrogen atoms were refined anisotropically. Hydrogen atoms were placed in calculated positions and refined using a riding model with fixed isotropic *U* values. There exists rotational disorder on a number of *t*-butyl groups in structures **4** (75:25 and 55:45) and **5** (75:25). Also, the disordered solvent regions in structures **4**, **5**, and **6** were treated in the manner described by van der Sluis and Spek,[10d] resulting in the removal of 149, 272, and 448 e^- per cell, respectively. These values approximate to $4CH_3OH$ (72), $4CH_3OH$ (72), and $14CH_3COCH_3$ (448 e^-) per formula unit, respectively. The data measurement and other refinement parameters for these five crystal structures are given in Table 1.

Spectroscopic Titrations. Spectrophotometric measurements in the UV−visible region were performed at 294 K using a CARY 100Bio UV−vis spectrophotometer and 1 cm path length matched quartz cuvettes. Chemicals and solvents were of AR grade unless otherwise stated and used as received. The "metal-only" complex **1** was dried in vacuo for 2 h prior to the preparation of the titration solutions, and the titrations were prepared immediately. Solutions of **1** in THF (2 mL, 1.5×10^{-5} mol L^{-1}) were titrated with THF solutions of the acid of interest (2.0×10^{-4} to 1.0×10^{-3} mol L^{-1}). The acid solutions were titrated at 0.20 molar equivalence increments for $HClO_4$, 0.25 molar equivalence increments for H_2SO_4 and HBr, and 1.0 molar equivalence increments for HNO_3. A 1:1 anion to **1** binding model was assumed except in the case of HBr where a 2:1 model was superior. Formation constants were calculated using the SPECFIT program (version 3.0.40, SPECFIT/32).[11] Titrations were repeated until three concordant results were obtained.

RESULTS AND DISCUSSION

Formation of "Metal-Only" Complex: [Cu$_2$(L^3-2H)$_2$], 1. Anion free charge-neutral dinuclear Cu(II) complex $[Cu_2(L^3\text{-}2H)_2]$, **1**, was readily isolated from the reaction of the ligand with copper acetate in a manner akin to that used previously.[7c] Microanalysis, ESMS, and X-ray structure determination all confirmed the general form of the complexes.

For X-ray analysis, dark green platelet shaped crystals of **1** were grown by slow diffusion of diisopropyl ether into a THF/$CHCl_3$ (1:1) mix of the complex. Figure 1 shows the molecular structure of complex **1** along with atom labeling scheme used. In stark contrast to $[Cu_2(L^2\text{-}2H)_2]$,[7c] the present complex $[Cu_2(L^3\text{-}2H)_2]$, **1**, does not form a helicate (Figure 2a). It consists of two Cu(II) ions coordinated to two dianionic L^3

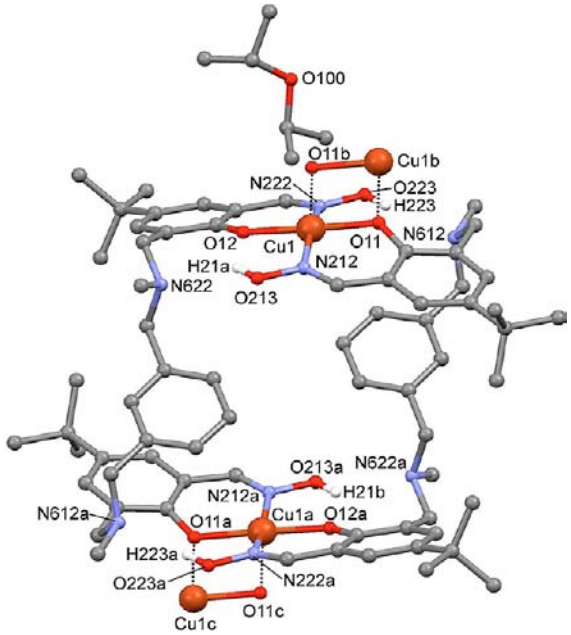

Figure 1. Perspective front view of complex **1** and the axially coordinated Cu−O of the adjacent complex molecules (non-hydrogen bonding hydrogen atoms have been omitted for clarity).

molecules with each copper sharing both ligands via phenolate and *N*-oximate coordination ($N_2O_2^{2-}$). The reduction in conformational freedom brought about by the 1,3-aryl linkers leads the complex to adopt a nonhelical, square parallelogram-type structure, where both phenolic rings on the ligand reside on the same side when the complex is viewed along the plane of the aryl groups in the straps (Figure 2a, RHS). The ligand confirmation is further stabilized by $\pi\cdots\pi$ stacking interactions between these aryl groups and the phenolic rings at the coordination sites with a centroid to centroid distance of 3.688(3) Å (Figure 2a, LHS). This nonhelical adopted conformation of the ligand is contrary to every other structure of this type to date.

The copper(II) centers are in a slightly distorted square pyramidal environment. The five donors consist of two nitrogen atoms (one oxime moiety from each ligand) and two oxygen atoms (one phenolate moiety from each ligand), and these contribute to the $N_2O_2^{2-}$ head to tail coordination mode of the in-plane donors. The fifth position consists of a coordinated phenolic oxygen atom in the axial position from a neighboring complex at a distance of 2.458(2) Å leading to the formation of a 1D polymeric chain along the *a* axis (Figure 2b). The Cu−O distances are 1.907(2) and 1.894(2) Å, and the Cu−N distances are 1.970(3) and 1.974(2) Å, which are consistent with similar complexes made previously.[7,8a] The axially coordinated arrangement between Cu1−O11b and Cu1b−O11 forms a parallelogram shaped coordination mode between the adjacent complex molecules (Figure 1). The important bond lengths and angles are summarized in Table 2. The in-plane donor/metal angles are all close to 180°, emphasizing the planarity of these donors, and the index parameter τ value of Cu1 is 0.22. This value of 22% distortion from square pyramidal toward a trigonal bipyramidal geometry indicates that the *m*-xylylic ligands bound to the metal centers in **1** cause a slightly more distorted square pyramidal geometry around the metal center than in $[Cu_2(L^2\text{-}2H)_2]$,[7c] which also has a distorted square pyramidal geometry with a τ value of

dx.doi.org/10.1021/ic400829d | Inorg. Chem. 2013, 52, 9327−9337

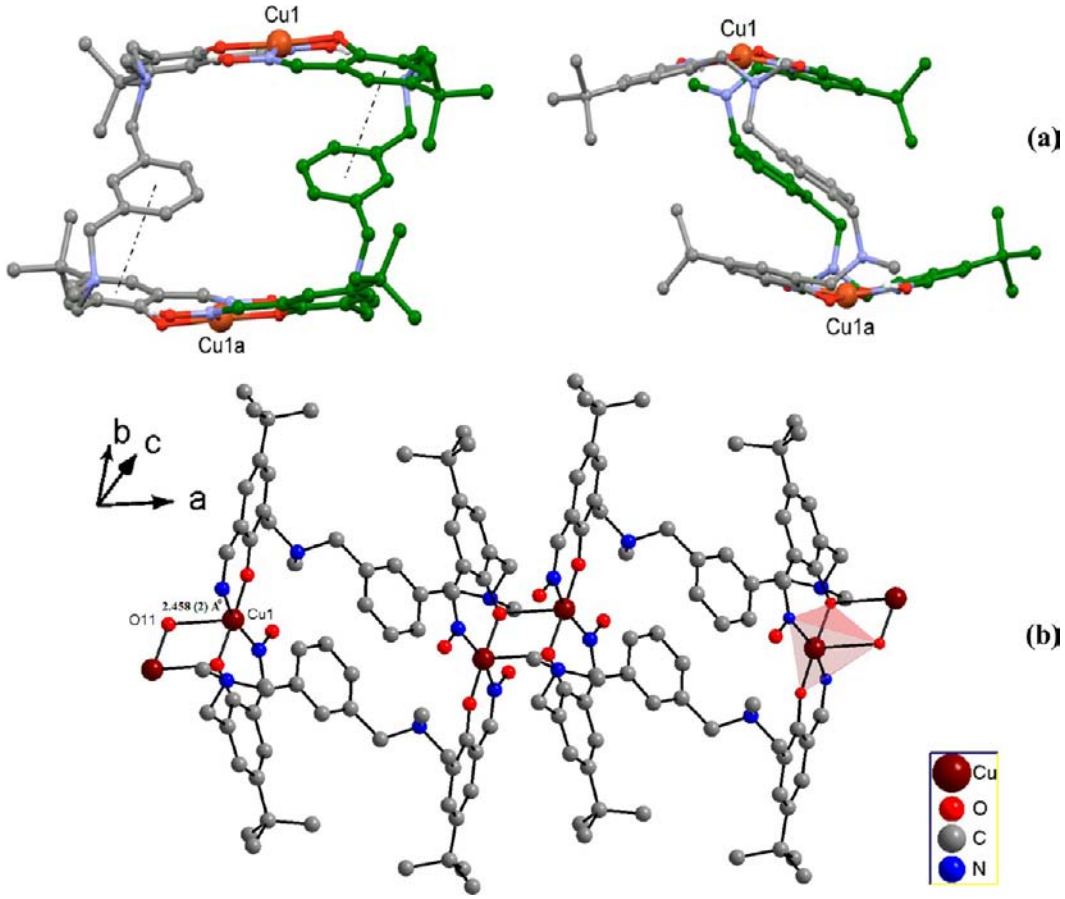

Figure 2. (a) Perspective front and side views of complex **1** showing the close $\pi-\pi$ stacking interactions and the edge-on positioning of the aryl rings in the strap (nonhelical strapping) and (b) the 1D polymeric chain. Also, the polyhedron (distorted square pyramid) around one of the copper(II) centers is shown.

Table 2. Selected Bond Lengths and Angles for the Cu(II) Centers in 1

atoms	bond lengths (Å)	X−Cu−X	bond angles (deg)
Cu1−O11	1.907(2)	O11−Cu−N212	91.57(9)
Cu1−O12	1.894(2)	O11−Cu−N222	90.01(9)
Cu1−N212	1.970(3)	O12−Cu−N222	90.40(9)
Cu1−N222	1.974(2)	O12−Cu−N212	87.77(9)
Cu1−O11b	2.458(2)	O11−Cu−O11b	82.62(3)
Cu1−Cu1a	8.854(1)		

17%. Thus, incorporation of the *m*-xylylic spacer, while affecting the structural conformation of the complex greatly (i.e., is not a helical complex), does not alter the inner sphere coordination environment of the copper metals. Each aromatic ring in the aryl linker exhibits $\pi-\pi$ interactions with an opposing phenolic ring from the same ligand. The ring-to-ring distances are 3.688 Å at an angle of 21.3°. This orientation of the aryl rings thus results in a significant reduction in void volume between the metal centers, and correspondingly the solvent molecule is located outside of the cavity, in contrast to $[Cu_2(\mathbf{L}^2\text{-}2H)_2]$.[7c]

Formation of Metal Salt Complexes. Cu(II) salt complexes containing the anions SO_4^{2-}, ClO_4^-, NO_3^-, and Br^- were readily prepared by direct combination of $\mathbf{L}^3$ and the appropriate Cu(II) salt in methanol. Crystals suitable for X-ray structure determination were obtained for $[NO_3\subset Cu_2\mathbf{L}^3_2](NO_3)_3$, **4**; $[2Br\subset Cu_2\mathbf{L}^3_2](Br)_2$, **5**; and $[2Br\subset(Cu_2\mathbf{L}^3_2)](BF_4)_2$, **6**, to determine the extent to which a restrictive strap might influence both anion binding and cavity geometries. Comparisons have also been made with previously published metal salt complexes of structurally related ligands $\mathbf{L}^1$ and $\mathbf{L}^2$.[7]

$[NO_3\subset(Cu_2\mathbf{L}^3_2)](NO_3)_3$ (4). Green rod-shaped crystals of complex **4** suitable for X-ray diffraction were grown by slow diffusion of diisopropyl ether into a methanol mix of the complex. Figure 3 shows the molecular structure of the complex. The asymmetric unit consists of one complete protonated complex with one encapsulated nitrate anion and three counter nitrate anion molecules. The two copper(II) centers are 6.662(3) Å apart and lying approximately above one another, linked by an intervening nitrate ion. The coordination environment for each copper atom is similar to anion free complex **1** mentioned above with both the metal centers coordinated to two $\mathbf{L}^3$ ligands through *N*-oximate and phenolate donors ($N_2O_2^{2-}$). Both of the Cu(II) centers are in the same environment due to the encapsulated NO_3^- anion possessing a weak bond to both metal centers, and there are no intermolecular bonds from either copper atom to any neighboring complex molecules. Cu1 and Cu2 have τ values of 0.23 and 0.31, respectively. These distorted square pyramidal environments around the metal centers are greater than was seen for the helicate complexes of *p*-xylylic ligand $\mathbf{L}^2$ (1,4 aryl linker based), $[Cu_2(\mathbf{L}^2\text{-}2H)_2]$, $[ClO_4\subset(Cu_2\mathbf{L}^2_2)](ClO_4)_3$, and $[BF_4\subset(Cu_2\mathbf{L}^2_2)](BF_4)_3$.[7c] This implies that the incorporated *m*-xylylic ligands (1,3 aryl linker-based) confer a more restrained geometry around the metal centers when in this helical

dx.doi.org/10.1021/ic400829d | *Inorg. Chem.* 2013, 52, 9327−9337

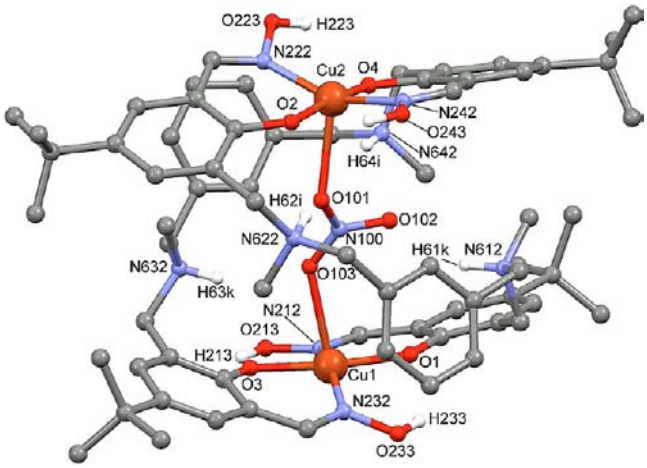

Figure 3. Perspective view of complex **4**, showing the NO_3^- anion encapsulated within the central cavity (non H-bonding hydrogen atoms, the disorder on the *t*-butyl groups on the salicylaldoxime rings O2 (75:25) and O4 (55:45) and the three counter nitrate anions have been omitted for clarity).

conformation. The Cu(II) centers have four donors that consist of two oxygen donors (one phenol moiety from each ligand) and two nitrogen donors (one oxime moiety from each ligand). The fifth bond in the axial position is with an oxygen atom of the nitrate anion, with bond distances of 2.441(6) and 2.401(6) Å for Cu1−O103 and Cu2−O101, respectively (Table 3).

Table 3. Selected Bond Lengths and Angles for the Cu(II) Centers in Complex 4

atoms	bond lengths (Å)	X−Cu−X	bond angles (deg)
Cu1−O1	1.890(4)	O1−Cu1−N212	92.32(17)
Cu1−O3	1.898(4)	O1−Cu1−N232	87.48(18)
Cu1−N212	1.961(5)	O3−Cu1−N212	91.59(17)
Cu1−N232	1.964(5)	O3−Cu1−N232	91.61(18)
Cu1−O103	2.441(6)	O1−Cu1−O103	94.31(12)
Cu2−O2	1.914(4)	O2−Cu2−N222	91.81(11)
Cu2−O4	1.893(4)	O2−Cu2−N242	89.99(19)
Cu2−N222	1.972(6)	O4−Cu2−N222	88.20(19)
Cu2−N242	1.935(6)	O4−Cu2−N242	93.22(19)
Cu2−O101	2.401(6)	O2−Cu2−O101	77.3(2)
		O1−Cu1−Cu2−O2	125.2(5)
Cu1−Cu2	6.6615(1)	O3−Cu1−Cu2−O4	125.8(3)

These are significantly shorter than a related copper−imine complex that also readily encapsulates a nitrate anion (Cu−O = 2.722(2) Å),[6b] suggesting that this helical complex has a smaller cavity available to the anion. A CCDC search for an average Cu−O (nitrate) bond length among similar systems was calculated to be 2.369 (3) Å.[12] A CCDC search for an average Cu−O(nitrate) bond length among similar systems was calculated to be 2.369 (3) Å.[12] This average distance is considerably shorter than that observed for the metal−anion bond lengths found in **4**, indicating that the nitrate anion is loosely held in the cavity and hence the bonds stretched.

The encapsulated nitrate has adopted a length wise orientation within the cavity and coordinates to both copper centers, maximizing the amount of strong interactions to the anion. These are two strong Cu−O bonds to the nitrate with bond distances of 2.441(6) and 2.401(6) Å to Cu1 and Cu2, respectively, and three moderate NH···O H-bonds with bond distances of 2.941(14), 3.009(8), and 3.066(9) Å to O102, O101, and O103, respectively (Table 3 and 4). This orientation

Table 4. Selected Intramolecular H-Bond Distances and Angles for Complex 4

atoms (D−H···A)	H-bond distances (Å)	D−H···A angles (deg)
N612−H61k···O102	2.941(14)	154.7
N622−H62i···O101	3.009(8)	153.6
N632−H63k···O103	3.066(9)	158.9
O233−H233···O1	2.661(6)	131.1
O213−H213···O3	2.838(6)	129.9
O243−H243···O2	2.713(6)	133.1
O223−H223···O4	2.706(6)	130.8
N612−H61k···O1	3.265(8)	115.2
N622−H62i···O2	2.869(8)	125.9
N632−H63k···O3	2.855(7)	124.0
N642−H64i···O4	3.131(8)	123.9

and increase in the number of stronger interactions to the captured nitrate is most likely due to the significant decrease in the Cu−Cu distance (6.6615(1) Å) as a result from the restricting *m*-xylylic spacers. This shorter distance between them allows the nitrate anion to coordinate to both metal centers. It is able to form this shorter Cu−Cu distance by increasing the helical twist of the linker ligand to give an average twist through the O−Cu−Cu−O angle of 125.5°. This is in comparison to our previously published ClO_4^- and BF_4^- complexes[7c] $[ClO_4\subset(Cu_2L^2_2)](ClO_4)_3$ and $[BF_4\subset(Cu_2L^2_2)](BF_4)_3$, which both have a slightly more twisted helix twist angle (4−5°) than **4** but have relatively longer Cu−Cu distances at 7.135 and 7.212 Å, respectively. This shows that this *m*-xylyl ligand system adopts a flatter arrangement between the copper coordination planes than does the *p*-xylyl linked system to encapsulate an anion.

The protonated tertiary amines of the aryl linker are angled toward the central cavity so as to increase the number of intermolecular H-bonds with the captured NO_3^- anion, with three moderate H-bonds having an average distance of 3.005 Å (Figure 4 and Table 4). Unlike the previously reported aryl strapped complexes $[ClO_4\subset(Cu_2L^2_2)](ClO_4)_3$ and $[BF_4\subset(Cu_2L^2_2)](BF_4)_3$, the encapsulated nitrate anion in complex **4** does not form anion−π interactions with the aryl rings of the linker strap. This is because the free oxygen atom on the nitrate anion is angled so as to be orientated toward, and forming a moderate H-bond to the protonated amine N612 instead (Figure 4). Clearly, the H-bond interaction dominates over the weaker anion−π interaction.

The pseudo macrocyclic cavity surrounding each metal center is completed by an oxime hydrogen bonded toward the opposing phenolate oxygen with an average OH···O distance of 2.730 (3) Å. This is the same as the average distance (2.731(3) Å) for the anion free complex **1**. This distance is slightly longer than the average distance for either the perchlorate complex $[ClO_4\subset(Cu_2L^2_2)](ClO_4)_3$ or the tetrafluoroborate complex $[BF_4\subset(Cu_2L^2_2)](BF_4)_3$, which shows that within complexes containing the more rigid aryl straps in a helical arrangement, these moderate strength interactions do not change appreciatively.[7c]

Within this complex **4** there also exists a secondary, weaker H-bond from the tertiary amines in the aryl linker to the phenolate oxygen atoms, with an average NH···O distance of

dx.doi.org/10.1021/ic400829d | Inorg. Chem. 2013, 52, 9327−9337

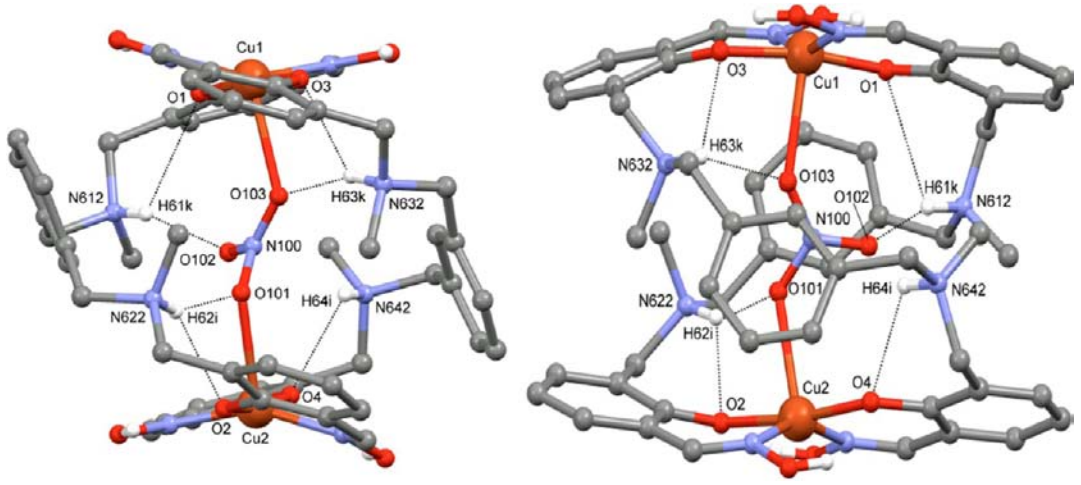

Figure 4. Perspective side-on views of the H-bonding of the protonated amines of the linker straps to the encapsulated nitrate anion and the phenolic oxygens in complex **4** (non-hydrogen bonding hydrogen atoms and the *t*-butyl groups have been omitted for clarity).

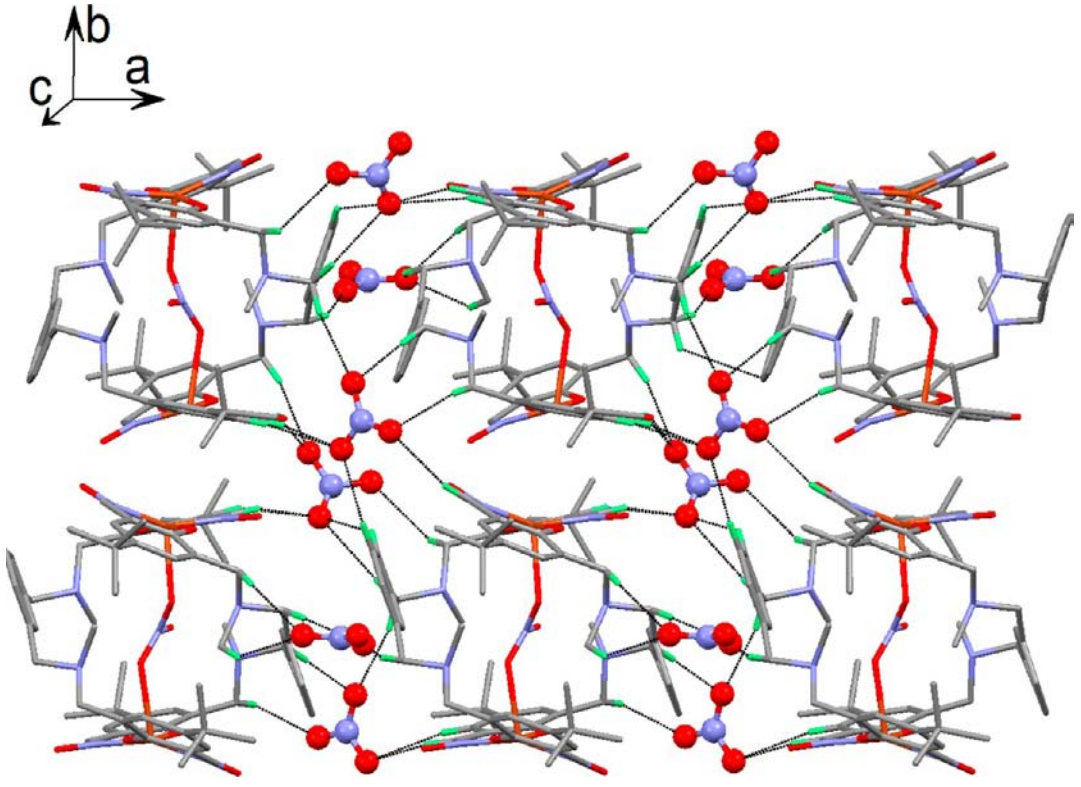

Figure 5. The H-bonded 2D sheet structure parallel to the *ab* plane formed by the nitrate ions present in the crystal lattice of complex **4**. The complex molecules are shown as capped sticks, while the nitrate ions are shown in ball and stick mode. The H-bonding interactions are shown as dotted lines, and H-atoms other than those involved in H-bonding are omitted for clarity. See also the Supporting Information.

2.907 Å, equivalent to the analogous distances in $[Cu_2(\mathbf{L}^3\text{-}2H)_2]\cdot 2C_6H_{14}O$, $[ClO_4\subset(Cu_2\mathbf{L}^2_2)](ClO_4)_3$, and $[BF_4\subset(Cu_2\mathbf{L}^2_2)](BF_4)_3$, again showing that this H-bond arrangement around the metal centers is unaltered regardless of changes at the anion binding site (Table 4). The counter nitrate anions are involved in many hydrogen bonds with the complex molecule and adjacent complexes. One of the nitrate counteranions (N300, O301, O302, O303) sits between three adjacent complexes and makes several mainly weak interactions. The second counter nitrate anion (N400, O401, O402, O403) is similar to N300 in that it is located near the oxime regions of the complex and of two other adjacent complexes, having only minor interactions to the surrounding complexes. The last counter nitrate anion (N200, O201, O202, O203) makes only weak interactions with an adjacent complex. These H-bonding interactions lead to the formation of a 2D sheet in the crystal lattice (Figure 5). The various parameters of these interactions are summarized in Table 5.

*$[2Br\subset(Cu_2L^3_2)](Br)_2$ (**5**).* Green block-shaped crystals of **5** suitable for X-ray diffraction were grown by slow diffusion of chloroform into a methanol/acetone (1:1) mix of the complex, and the crystal structure was determined (Figure 6). The asymmetric unit consists of one complete protonated complex with two coordinated bromide anions, two counter bromide

dx.doi.org/10.1021/ic400829d | *Inorg. Chem.* 2013, 52, 9327−9337

Table 5. H-Bonding Parameters for 2D Sheet Structure Formed in Case of Complex 4[a]

atoms (D−H···A)	H-bond distance (Å)	D−H···A angle (deg)
C34−H34A···O302[i]	2.608	147
C241−H24A···O302[i]	2.530	150
C614−H61F···O401[i]	2.823	178
C641−H64B···O301[ii]	2.581	118
C638−H63J···O302[ii]	2.693	137
C644−H64F···O302[ii]	2.608	156
C644−H64G···O401[ii]	2.580	164
C211−H21A···O402[ii]	2.455	158
C31−H31A···O402[ii]	2.660	150
C213−H213···O303[iii]	2.197	125
C631−H63A···O303[iii]	2.597	166
C637−H637···O402[iv]	2.642	175
C624−H62G···O202[v]	2.657	171
C623−H62E···O203[v]	2.621	141
C624−H62G···O203[v]	2.634	141
C621−H62A···O203[v]	2.427	143
C634−H63G···O202[vi]	2.473	152

[a]Symmetry equivalents: i = *x*, *y*, *z*; ii = *x* + 1, +*y*, +*z*; iii = −*x*, +*y* + 1/2, −*z*; iv = −*x*, +*y* − 1/2, −*z*; v = *x*, +*y*, +*z* + 1; vi = *x* + 1, +*y*, +*z* + 1.

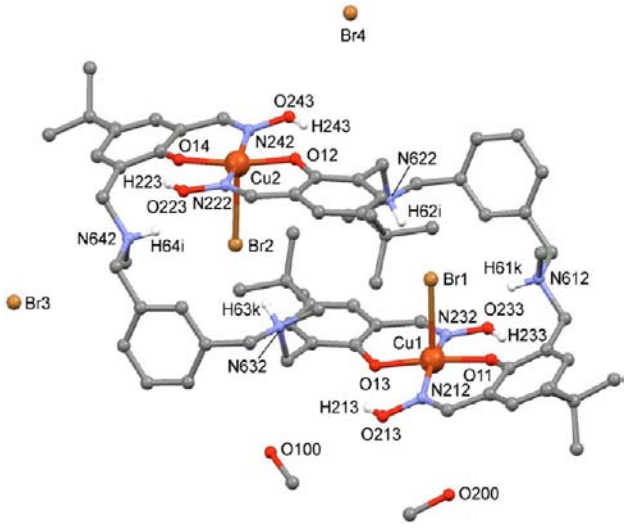

Figure 6. Perspective view of complex **5**, the counter bromide anions, and the methanol solvent molecules (hydrogen atoms not involved in H-bonding and the disorder on the *t*-butyl group on the salicylaldoxime ring O14 (75:25) have been omitted for clarity).

anions, and two methanol solvent molecules. Each tertiary amine is protonated giving rise to an overall neutral complex. The complex consists of two Cu(II) atoms coordinated to two L^3 molecules in the zwitterionic form (phenolate/ammonium) with each copper center bound to *N*-oximate and *O*-phenolate donors from each ligand in a head to tail coordination mode.

The Cu(II) centers in **5** are in slightly differing environments. Both Cu1 and Cu2 are in a slightly distorted square pyramidal arrangement. Their corresponding τ values are 0.13 and 0.05, respectively. These τ values show how close the metal centers are to true square pyramidal geometry and are the least distorted square pyramidal geometries seen within these xylylic family of complexes made.

The Cu(II) metal centers both have five donors in common, which consist of two oxygen donors (one phenol moiety from each ligand), two nitrogen donors (one oxime moiety from each ligand), and the fifth being a coordinated bromide anion in the axial position at a distance of 2.782(1) Å for Cu1−Br1 and 2.765(1) Å for Cu2−Br2. Cu1 also possesses a very weak bonding interaction to a phenolate oxygen from an adjacent complex at a distance of 3.2027(1) Å (Table 6). This brings the copper centers of adjacent complexes relatively close, at a distance of 3.8720(1) Å for Cu1−Cu2b.

Table 6. Selected Bond Lengths and Angles for the Cu(II) Centers in Complex 5

atoms	bond lengths (Å)	X−Cu−X	bond angles (deg)
Cu1−Br1	2.782(1)	O11−Cu1−Br1	86.04(8)
Cu1−O11	1.923(2)	O11−Cu1−N212	90.99(11)
Cu1−O13	1.918(2)	O11−Cu1−N232	87.59(11)
Cu1−N212	1.964(3)	O13−Cu1−N212	88.70(11)
Cu1−N232	1.953(3)	O13−Cu1−N232	91.17(11)
Cu1−O14b	3.2027(1)	O11−Cu1−O14b	93.32(11)
Cu2−Br2	2.765(1)	O14−Cu2−Br2	88.44(9)
Cu2−O12	1.914(2)	O14−Cu2−N242	91.11(12)
Cu2−O14	1.913(2)	O14−Cu2−N222	88.35(11)
Cu2−N222	1.948(3)	O12−Cu2−N222	91.50(12)
Cu2−N242	1.966(3)	O12−Cu2−N242	87.28(12)

A CCDC search revealed that square pyramidal Cu(II) complexes with a bromide coordinated in the axial position have an average Cu−Br bond distance (2.699 (4) Å) slightly shorter than those found for **5**.[13] This slight lengthening of the Cu−Br bond distance in **5** from the average is most likely due to the additional H-bonding and close contact interactions from the ligand to the bromine atom from within the complex; essentially a pocket has been formed in which the bromine atom is stabilized via multiple covalent, electrostatic, and H-bonding interactions (Figure 7 and Table 7). Obviously Cu−Br coordination is not unique in copper chemistry; however, within the context of copper oxime-based helical complexes this 1:1:1, Cu:Br:ligand structural arrangement is an exception to every previous example we have structurally characterized with the helical shape adopted when the nitrate salt was used the status quo for a wide range of anions (Figure 3). The reason for this change in structural morphology is a direct consequence of the conformationally restrictive *m*-xylylic groups now incorporated into the linker. This coupled with the different size, charge density, and coordination nature of the Br^- anion provides an alternative structural motif, with the resulting shape approximating a distorted rectangular box (Figure 6). There appears to be a subtle balance between anion influence and conformational freedom in effect here. In the presence of this restrictive *m*-xylylic linker, the bridging bidentate coordination nature of the nitrate anion with a bigger bite length[14] enables it to link the two copper(II) centers in complex **4**, thus forcing the ligand straps to wind around each other and form the dihelicate structure. On the other hand, in complex **5**, the monatomic bromide anion possesses a bite length too small to affect this change and instead adopts a monodentate coordination mode to each of the two Cu(II) centers. In an effort to minimize the electrostatic interactions between the two bromide entities within the cavity while simultaneously maximizing the H-bonding interactions with the nearby ammonium groups, the molecule adopts an elongated conformation. The copper(II) centers are now lying diagonally across from one another with the Cu···Cu distance stretched to

dx.doi.org/10.1021/ic400829d | *Inorg. Chem.* 2013, 52, 9327−9337

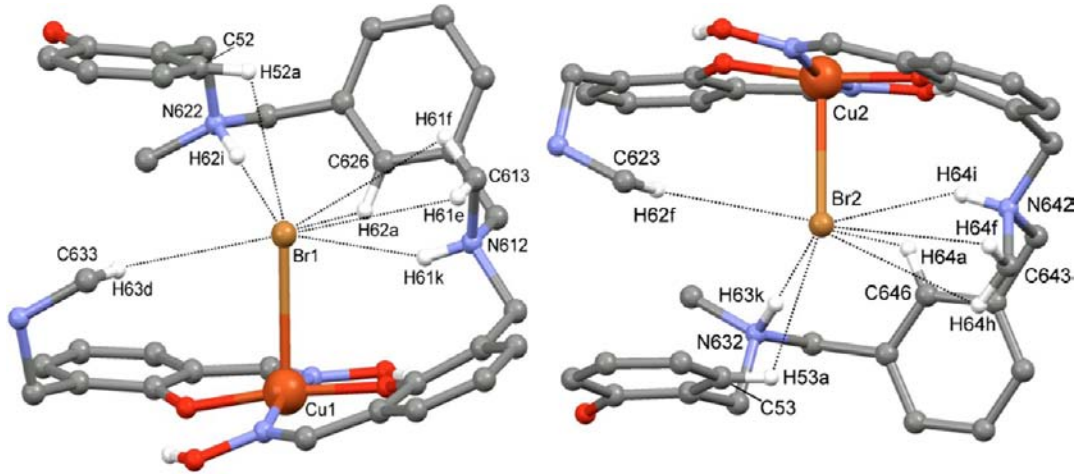

Figure 7. Partial perspective views of the binding pockets in complex **5**, showing the H-bonding and close contact hydrogens surrounding the coordinated Br1 and Br2 (hydrogen atoms not involved in H-bonding or in close contact to Br1 or Br2 and the *t*-butyl groups have been omitted for clarity).

Table 7. Selected H-Bonds and Close Contact Distances and Angles for the Bound Bromide Anions in Complex 5

atoms (D−H···A)	H-bond distances (Å)	D−H···A angles (deg)
Br1		
N612−H61k···Br1	3.498(3)	151.6
N622−H62i ···Br1	3.311(3)	173.6
C613−H61e···Br1	3.738(4)	88.5
C613−H61f···Br1	3.738(4)	99.4
C633−H63d···Br1	3.761(4)	120.7
C52−H52a ··· Br1	3.432(4)	106.9
C626−H62a···Br1	3.477(3)	109.1
Br2		
N632−H63k···Br2	3.300(3)	177.6
N642−H64i···Br2	3.497(3)	147.9
C643−H64f···Br2	3.677(4)	87.1
C643−H64h···Br2	3.677(4)	102.4
C623−H62f···Br2	3.764(4)	120.4
C53−H53a···Br2	3.502(4)	106.5
C646−H64a···Br2	3.429(4)	101.4

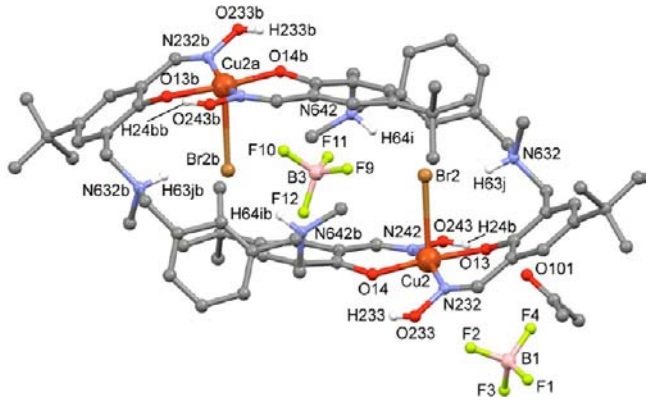

Figure 8. Perspective view of one complex within the unit cell, two of the counter tetrafluoroborate anions, and an acetone solvent molecule in complex **6** (hydrogen atoms not involved in H-bonding and the disorder on the tetrafluoroborate anion B3 (74:26) have been omitted for clarity).

8.778(3) Å. The charge balance for complex **5** is completed by two noncoordinating bromides, which have no significant interactions with the complex.

In a further experiment, the conditions of the reaction were altered to a 1:1:0.5 ratio of $\mathbf{L}^3$:$Cu(BF_4)_2$:TBABr in an attempt to favor the mono anion encapsulated helicate structural form, analogous to that of the nitrate structure **4**. However, when the molecular structure of the complex **6** was investigated, it was found that the resulting structure was very similar to **5** with the exception that the counterions had now been replaced by two BF_4^- anions situated around the complex.

*[2Br⊂(Cu$_2$**L**$^3_2$)](BF$_4$)$_2$* ***(6)***. Green chunk-shaped crystals of complex **6** suitable for X-ray diffraction were grown by slow diffusion of diethyl ether into a methanol/acetone (1:1) mix of the complex, and the crystal structure was determined (Figure 8). The asymmetric unit consists of three half complexes with the other halves generated by inversion, six tetrafluoroborate counteranions, and two acetone solvent molecules. This complex is structurally similar to the previous bromide complex **5** discussed above having the same flattened rectangular "box" structure, but contains slightly different bond lengths and angles and a different packing arrangement in the crystal lattice. This complex also consists of two Cu(II) ions coordinated to two protonated $\mathbf{L}^3$ molecules (at the tertiary amines) with each copper center sharing both ligands via the *N*-oximate and the *O*-phenolate positions, again forming the head to tail coordination mode. The Cu(II) centers in **6** are in the same square pyramidal environments. The τ values of the metal centers are Cu1 = 0.29, Cu2 = 0.25, and Cu3 = 0.31. These high τ values indicate that the Cu(II) centers for **6** are in more distorted square pyramidal geometries when compared to the equivalent geometries in **5**. This higher distortion of the metal centers in the crystal lattice maybe an indirect consequence of the different packing arrangement now present in **6** (BF_4^- counteranions) when compared to **5** (Br^- counteranions). Both copper centers have five donors in common that consist of two oxygen donors (one phenolate moiety from each ligand) and two nitrogen donors (one oxime moiety from each ligand). The fifth position is a coordinated bromide in the axial position, with a Cu1−Br1 distance of 2.734(2) Å, a Cu2−Br2 bond distance of 2.778(2) Å, and a Cu3−Br3 bond distance of 2.734(2) Å (Table 8). The Cu−Br bond lengths found in **6** are comparable to those in **5** and are also slightly longer than the

dx.doi.org/10.1021/ic400829d | *Inorg. Chem.* 2013, 52, 9327−9337

Table 8. Selected Bond Lengths and Angles for the Cu(II) Centers in Complex 6

atoms	bond lengths (Å)	X−Cu−X	bond angles (deg)
Cu1−Br1	2.734(2)	O11−Cu1−Br1	87.67(19)
Cu1−O11	1.934(8)	O11−Cu1−N212	91.0
Cu1−O12	1.946(8)	O11−Cu1−N222	86.8(4)
Cu1−N212	1.99(1)	O12−Cu1−N212	87.8(5)
Cu1−N222	2.03(1)	O12−Cu1−N222	92.5(5)
Cu2−Br2	2.778(2)	O13−Cu2−Br2	85.2(5)
Cu2−O13	1.935(9)	O13−Cu2−N232	90.2(5)
Cu2−O14	1.927(8)	O13−Cu2−N242	90.5(4)
Cu2−N232	1.95(1)	O14−Cu2−N232	86.0
Cu2−N242	2.01(1)	O14−Cu2−N242	92.1(4)
Cu3−Br3	2.734(2)	O15−Cu3−Br3	97.5(5)
Cu3−O15	1.929(8)	O15−Cu3−N252	90.2(5)
Cu3−O16	1.909(8)	O15−Cu3−N262	89.7(5)
Cu3−N252	1.94(1)	O16−Cu3−N252	87.9(5)
Cu3−N262	1.94(1)	O16−Cu3−N262	90.3(5)

average (2.699 Å) found for other similar complexes.[13] The acetone solvent molecule is located near an oxime functionality of the complex. O101 has a moderate H-bond to an oxime OH group H24b at a distance of 2.95(2) Å.

Anion Binding Studies. The "copper-only" complex **1** was subjected to titrations with a variety of acids in THF, and the changes to the electronic properties of the phenolate $\pi\rightarrow\pi^*$ transition were monitored by UV−vis spectroscopy. This was done to quantify the effect that the more restricting *m*-xylylic linker might play with regards to anion affinity of the receptor. Binding constant data are given in Table 9 along with the

Table 9. Showing the Formation Constants for "Metal-Only Complexes" $[Cu_2(L^3\text{-}2H)_2$ and $[Cu_2(L^2\text{-}2H)_2$[7c] Obtained from Spectroscopic Titrations with H_2SO_4, $HClO_4$, HBr, and HNO_3 in THF at 294 K

acid	log *K* $[C_2(L^3\text{-}2H)_2$	log *K* $[Cu_2(L^2\text{-}2H)_2$[7c]
H_2SO_4	4.49 ± 0.15	5.53 ± 0.32
$HClO_4$	4.61 ± 0.06	3.86 ± 0.22
HNO_3	3.76 ± 0.07	3.72 ± 0.08
HBr	4.61 ± 0.07 (2:1)	3.69 ± 0.17

previously reported values for the *p*-xylylic linked receptor[7c] for the purposes of comparison. Immediately it is apparent that in the case of **1** the data are not consistent with the previously observed trend for these family of complexes where stability of the anion encapsulated complex $[X^{n-}\subset Cu_2L^3_2]^{(4-n)+}$ is dependent upon a combination of anion charge and metal coordination ability. In fact, complex **1** was found to have an unexpected optimum 1:1 stability constant for the perchlorate anion, possibly as a result of the more restricting *m*-xylylic linker creating a more conserved, smaller cavity, favoring stronger interactions with the smaller anion. Indirect evidence for this tighter cavity comes from the structure determination of the nitrate encapsulated complex where the nitrate is bound to both copper atoms within the complex, a feature not observed in the related nitrate encapsulated hexyl linked dicopper complex, in which there were no metal anion bonds present.[6b] A 2:1 ratio of anion to complex has been observed for the first time in this class of complexes. This double loading of bromide is stabilized by the multitude of H-bonds, electrostatic interactions, and direct coordination to the Cu(II) centers. On the basis of the observed binding data, the receptor **1** with a 1,3-xylyl linkage has enhanced affinity for the bromide anion over the analogous 1,4-xylyl receptor. Interestingly, this comes at the expense of the ability to bind sulfate as **1** now appears to be detuned for this anion. The stability constants of both **1** and $[Cu_2(L^2\text{-}2H)_2]$[7c] with nitrate are the same. This is most likely due to the typically noncoordinating nature of the nitrate anion in addition to its smaller size, meaning it has longer contact distances to the protonated amines and the aryl π systems, resulting in equally weak binding within either complex cavity. Amendola et al. have recently reported a relationship between anion size and choice of xylyl linker in ion selective studies on azacryptands.[15] They demonstrated that the *p*-xylyl cryptand cavity is more suitable to host large anionic guests such as perrhenate, perchlorate, and iodide, despite their low density charge. On the contrary, nitrate, bromide, and chloride were shown to fit better into the smaller cavity of the *m*-xylyl cryptand. The higher affinity of the *m*-xylyl cage toward chloride over that of perrhenate was also demonstrated by the crystal structure of the 1:1 adduct.

CONCLUSIONS

With a slight modification in the aryl linker, essentially replacing a 1,4-aryl spacer[7c] with a 1,3-aryl one, there now exists increased structural rigidity within the complexes formed. In addition, this resulted in the formation of new conformers, which are dependent on anion choice. The anion free receptor **1** displays a nonhelical structure in the absence of anions, a contracted helical complex upon encapsulation of nitrate in complex **4**, and finally a nonhelical rectangular "box" type 2:1 binding complex with bromide anions in complexes **5** and **6**. This complete turnabout in structural conformation and flexibility by way of the *m*-xylylic linker is further exemplified in the anion binding results. It has resulted in a dramatic change in binding strength of the same anions under the same conditions when compared to the analogous *p*-xylylic linker. Presuming a comparison for a 1:1 ratio of anion to complex **1**, the perchlorate anion now exhibits the strongest binding, while this complex is also now capable of double loading the Br^- anion with an estimated relatively high log K_1 binding strength comparable to the perchlorate and sulfate anions. The ability to bind nitrate appears unaffected and is not dependent on the linkage. In a nutshell, the use of a linkage that imparts restrictions on the resulting complexes also appears to offer an opportunity for anions themselves to have an influence on the resulting complex geometry and structure.

The synthesis, structure, and binding studies of these salicylaldoxime-based ditopic receptors systems involving both cations as well as anions promises to be an interesting field of research. Further variation in the linker and the influence of anions in the resulting complexes continues to be something we are actively pursuing, as is the influence of transition metals capable of octahedral coordination on the structural arrangements of these ligands.

ASSOCIATED CONTENT

Supporting Information

Crystallographic data (CIF files CCDC 926413−926417), UV−visible spectra for acid addition to anion free complex $[Cu_2(L^3\text{-}2H)_2]$, **1**, and pictorial descriptions of the H-bonding interactions involving the nitrate anions in $[NO_3\subset(Cu_2L^3_2)]\text{-}(NO_3)_3$, **4** . This material is available free of charge via the Internet at http://pubs.acs.org.

dx.doi.org/10.1021/ic400829d | *Inorg. Chem.* 2013, 52, 9327−9337

AUTHOR INFORMATION

Corresponding Author

*Tel.: 0064 6 356 9099, ext 7825. Fax: 0064 6 350 5682. E-mail: p.g.plieger@massey.ac.nz.

Notes

The authors declare no competing financial interest.

ACKNOWLEDGMENTS

We wish to thank Professor Geoffrey Jameson for his help with the structural refinement of structure **6**. P.G.P. would like to acknowledge the financial assistance from the Massey University Research Fund. A.P.S.P. would like to acknowledge Massey University for the Post-Doctoral fellowship. For the high-resolution mass spectroscopy data of **2**, we thank Mrs. Pat Gread and Professor Bill Henderson from the University of Waikato.

REFERENCES

(1) Park, C. H.; Simmons, H. E. *J. Am. Chem. Soc.* **1968**, *90*, 2431−2432.

(2) (a) Graf, E.; Lehn, J.-M. *J. Am. Chem. Soc.* **1976**, *98*, 6403−6405. (b) Schmidtchen, F. P. *Angew. Chem., Int. Ed. Engl.* **1977**, *16*, 720−721.

(3) (a) Llinares, J. M.; Powell, D.; Bowman-James, K. *Coord. Chem. Rev.* **2003**, *240*, 57−75. (b) Sessler, J. L.; Gale, P. A.; Cho, W.-S. *Anion Receptor Chemistry*; Royal Society of Chemistry: Cambridge, UK, 2006. (c) Philip, A. G. *Anion Recognition in Supramolecular Chemistry*; Springer Science: New York, 2010. (d) Stibor, I.; Anslyn, E. V. *Anion Sensing*; Springer Science: New York, 2005. (e) Bianchi, A.; Bowman-James, K.; García-España, E. *Supramolecular Chemistry of Anions*; Wiley-VCH: New York, 1997. (f) Schmidtchen, F. P.; Berger, M. *Chem. Rev.* **1997**, *97*, 1609−1646. (g) Rice, C. R. *Coord. Chem. Rev.* **2006**, *250*, 3190−3199.

(4) Gale, P. A. *Coord. Chem. Rev.* **2000**, *199*, 181−233. (b) Chrisstoffels, L. A. J.; Jong, F.; Reinhoudt, D. N.; Sivelli, S.; Gazzola, L.; Casnati, A.; Ungaro, R. *J. Am. Chem. Soc.* **1999**, *121*, 10142−10151.

(5) (a) Mahoney, J. M.; Stucker, K. A.; Jiang, H.; Carmichael, I.; Brinkmann, N. R.; Beatty, A. M.; Noll, B. C.; Smith, B. D. *J. Am. Chem. Soc.* **2005**, *127*, 2922−2928. (b) Cametti, M.; Nissinen, M.; Cort, A. D.; Mandolini, L.; Rissanen, K. *J. Am. Chem. Soc.* **2005**, *127*, 3831−3837. (c) He, X.; Yam, V. W. *Inorg. Chem.* **2010**, *49*, 2273−2279. (d) Cametti, M.; Ilander, L.; Valkonen, A.; Nieger, M.; Nissinen, M.; Nauha, E.; Rissanen, K. *Inorg. Chem.* **2010**, *49*, 11473−11484. (e) Riis-Johannessen, T.; Schenk, K.; Severin, K. *Inorg. Chem.* **2010**, *49*, 9546−9553. (f) Shanmugaraju, S.; Bar, A. K.; Chi, K.; Mukherjee, P. S. *Organometallics* **2010**, *29*, 2971−2980. (g) Xie, Y.; Mak, T. C. W. *J. Am. Chem. Soc.* **2011**, *133*, 3760−3763. (h) Devoille, A. M. J.; Richardson, P.; Bill, N. L.; Sessler, J. L.; Love, J. B. *Inorg. Chem.* **2011**, *50*, 3116−3126. (i) Clever, G. H.; Kawamura, W.; Shionoya, M. *Inorg. Chem.* **2011**, *50*, 4689−4691.

(6) (a) Plieger, P. G.; Parsons, S.; Parkin, A.; Tasker, P. A. *J. Chem. Soc., Dalton Trans.* **2002**, 3928−3930. (b) Wenzel, M.; Bruere, S. R.; Knapp, Q. W.; Tasker, P. A.; Plieger, P. G. *Dalton Trans.* **2010**, *39*, 2936−2941.

(7) (a) Wenzel, M.; Jameson, G. B.; Ferguson, L. A.; Knapp, Q. W.; Forgan, R. S.; White, F. J.; Parsons, S.; Tasker, P. A.; Plieger, P. G. *Chem. Commun.* **2009**, 3606−3608. (b) Wenzel, M.; Knapp, Q. W.; Plieger, P. G. *Chem. Commun.* **2011**, *47*, 499−501. (c) Stevens, J. R.; Plieger, P. G. *Dalton Trans.* **2011**, *40*, 12235−12241.

(8) (a) Wenzel, M.; Forgan, R. S.; Faure, A.; Mason, K.; Tasker, P. A.; Piligkos, S.; Brechin, E. K.; Plieger, P. G. *Eur. J. Inorg. Chem.* **2009**, 4613−4617. (b) Mason, K.; Chang, J.; Prescimone, A.; Garlatti, E.; Carretta, S.; Tasker, P. A.; Brechin, E. K. *Dalton Trans.* **2012**, *41*, 8777−8785.

(9) (a) Vilar, R. *Angew. Chem., Int. Ed.* **2003**, *42*, 1460−1477. (b) Campos-Fernández, C. S.; Schottel, B. L.; Chifotides, H. T.; Bera, J. K.; Bacsa, J.; Koomen, J. M.; Russell, D. H.; Dunbar, K. R. *J. Am. Chem. Soc.* **2005**, *127*, 12909−12923. (c) Kim, H.; Zin, W.; Leem, M. *J. Am. Chem. Soc.* **2005**, *126*, 7009−7014. (d) Spence, G.; Beer, P. *Acc. Chem. Res.* **2013**, *46*, 571−586. (e) Kato, M.; Fujihara, V.; Yanoc, D.; Nagasawaa, A. *CrystEngComm* **2008**, *10*, 1460−1466. (f) Awaleh, M. O.; Badia, A.; Brisse, F. *Inorg. Chem.* **2007**, *46*, 3185−3191. (g) Awaleh, M. O.; Badia, A.; Brisse, F.; Bu, X.-H. *Inorg. Chem.* **2006**, *45*, 1560−1574. (h) Awaleh, M. O.; Badia, A.; Brisse, F. *Cryst. Growth Des.* **2006**, *6*, 2674−2685. (i) Awaleh, M. O.; Badia, A.; Brisse, F. *Inorg. Chem.* **2005**, *44*, 7833−7845. (j) Bu, X. H.; Xie, Y. B.; Li, J. R.; Zhang, R. H. *Inorg. Chem.* **2003**, *42*, 7422−7430.

(10) (a) Rigaku. *CrystalClear, Version 1.4.0*; Rigaku Americas Corp.: The Woodlands, TX, 2005. (b) Rigaku. *PROCESS-AUTO*; Rigaku Corp.: Tokyo, Japan, 1998. (c) Sheldrick, G. M. *Acta Crystallogr.* **2008**, *A64*, 112−122. (d) van der Sluis, P.; Spek, A. L. *Acta Crystallogr., Sect. A* **1990**, *46*, 194−201.

(11) (a) Gampp, H.; Maeder, M.; Meyer, C. J.; Zuberbuehler, A. d. *Talanta* **1985**, *32*, 95−101. (b) Gampp, H.; Maeder, M.; Meyer, C. J.; Zuberbuehler, A. d. *Talanta* **1985**, *32*, 257−264. (c) Gampp, H.; Maeder, M.; Meyer, C. J.; Zuberbuehler, A. d. *Talanta* **1985**, *32*, 1133−1139.

(12) (a) Albada, G. A.; Dominicus, I.; Mutikainen, I.; Turpeinen, U.; Reedijk, J. *Polyhedron* **2007**, *26*, 3731−3736. (b) Albada, G. A.; Horst, M. G.; Mutikainen, I.; Turpeinen, U.; Reedijk, J. *Inorg. Chim. Acta* **2008**, *361*, 3380−3387. (c) Biswas, C.; Drew, M. G. B.; Ruiz, E.; Estrader, M.; Diaz, C.; Ghosh, A. *Dalton Trans.* **2010**, *39*, 7474−7484. (d) Ruffer, T.; Brauer, B.; Powell, A. K.; Hewitt, I.; Salvan, G. *Inorg. Chim. Acta* **2007**, *360*, 3475−348. (e) Carlucci, L.; Ciani, G.; Gramacciolo, A.; Proserpio, D. M.; Rizzato, S. *CrystEngComm* **2000**, *29*, 1−10. (f) Ferrer, S.; Koningsbruggen, P. J.; Haasnoot, J. G.; Reedijk, J.; Kooijman, H.; Spek, A. L.; Lezama, L.; Arif, A. M.; Miller, J. S. *J. Chem. Soc., Dalton Trans.* **1999**, 4269−4276. (g) Li, N.; Chen, S.; Gao, S. *J. Coord. Chem.* **2007**, *60*, 117−123. (h) Ulku, D.; Tatar, L.; Atakol, O.; Durmus, S. *Acta Crystallogr.* **1999**, *C55*, 1652−1654. (i) Das, S.; Madhavaiah, C.; Verma, S.; Bharadwaj, P. K. *Inorg. Chim. Acta* **2005**, *358*, 3236−3240. (j) Vaiana, L.; Mato-Iglesias, M.; Esteban-Gomez, D.; Platas-Iglesias, C.; Blas, A.; Rodriguez-Blas, T. *Polyhedron* **2010**, *29*, 2269−2277.

(13) (a) Singh, P.; Copeland, V. C.; Hatfield, W. E.; Hodgson, D. J. *J. Phys. Chem.* **1972**, *76*, 2887−2891. (b) Thompson, L. K.; Mandel, S. K.; Gabe, E. J.; Lee, F. L.; Addison, A. W. *Inorg. Chem.* **1987**, *26*, 657−664. (c) Mandal, S. K.; Thompson, L. K.; Newlands, M. J.; Gabe, E. J.; Nag, K. *Inorg. Chem.* **1990**, *29*, 1324−1327. (d) He, Z.; Chaimungkalanont, J.; Craig, D. C.; Colbran, S. B. *Dalton Trans.* **2000**, 1419−1429. (e) Du, M.; Guo, Y.; Bu, X. *Inorg. Chim. Acta* **2002**, 136−140. (f) Yang, B.; Zeng, H.; Dong, Z.; Mao, J. *J. Coord. Chem.* **2003**, *56*, 1513−1523. (g) Telfer, S. G.; Parker, N. D.; Kuroda, R.; Harada, T.; Lefebvre, J.; Leznoff, D. B. *Inorg. Chem.* **2008**, *47*, 209−218.

(14) Amendola, V.; Fabbrizzi; Mangano, C.; Pallavicini, P.; Poggi, A.; Taglietti, A. *Coord. Chem. Rev.* **2001**, *219−221*, 821−837.

(15) Amendola, V.; Alberti, G.; Bergamaschi, G.; Biesuz, R.; Boiocchi, M.; Ferrito, S.; Schmidtchen, F. *Eur. J. Inorg. Chem.* **2012**, *21*, 3410−3417.